Geotextiles and Geomembranes 45 (2017) 161–168

Contents lists available at ScienceDirect

Geotextiles and Geomembranes

journal homepage: www.elsevier.com/locate/geotexmem

Experimental evaluation of geosynthetics as reinforcement for shotcrete

R. Moffat [a, *], C. Jadue [b], J.F. Beltran [c], R. Herrera [c]

[a] Department of Civil Engineering, Universidad Adolfo Ibañez, Santiago, Chile
[b] Petrus Geotechnical Consulting, Dr. Roberto del Rio 1245, Providencia, Santiago, Chile
[c] Department of Civil Engineering, University of Chile, Blanco Encalada 2002, Santiago, Chile

ARTICLE INFO

Article history:
Received 5 May 2015
Received in revised form
4 January 2017
Accepted 4 January 2017
Available online 17 February 2017

Keywords:
Geosynthetics
Shotcrete
Geosynthetics reinforcement
Energy absorption
Shotcrete strength

ABSTRACT

One of the commonly used stabilization systems for rock tunnels is shotcrete. This fine aggregate mortar is usually reinforced for improving its tensile and shear strength. In deep tunnels, its capacity to absorb energy has been recently considered for design purposes, as large displacements of the wall are expected. Two of the most used materials of reinforcement are steel welded-wire mesh and fibers (steel or polypropylene) in the shotcrete mix. This study presents the results and discussion of an experimental test program conducted to obtain the load-deformation curves of reinforced shotcrete, according to ASTM C 1550, using geosynthetics grids and geotextiles as alternative reinforcement materials. In addition, plain shotcrete and steel welded-wire mesh reinforced shotcrete specimens are also considered in the experimental program as benchmark cases. The experimental results are analyzed in terms of maximum strength and toughness. Results show that the use of geosynthetics as a reinforcement material is a promising alternative to obtain shotcrete with energy absorption capacity comparable with the most common reinforcement materials used.

1. Introduction

Shotcrete has been used for more than 50 years in ground support applications. Before 1990 only a few research works had been published in scientific journals (Franzen, 1992) in which the main information reported was related to the mechanical properties of the shotcrete with little emphasis on how to consider the use of this material on the improvement of the safety of a tunnel. Some of the main design principles for ground supports are to sustain the loads and deformations that the ground may induce during a tunnel's working life, maintain adequate stability of the ground, and protect workers and equipment against rock falls (Hoek et al., 2000; The British Tunneling Society & The Institution of Civil Engineers (2004); Malmgren, 2005). The interaction between rock and shotcrete, however, is a complex issue. The performance, and consequently the load carrying capacity and deformability of the shotcrete, is influenced by a number of factors such as: the mechanical properties of the rocks, the rock stresses, the presence of rock bolts, the interface between rock and shotcrete, and the mechanical properties and thickness of the shotcrete among others (Hoek et al., 2000; Malmgren, 2005; Ansell, 2010; Austin and Robins, 1995; Galli et al., 2004). Hence, due to this complex interaction behavior, a combination of empirical (Bieniawski, 1994; Barton et al., 1974; Palmstrom, 1996) and analytical methods (Wood, 1975; Einstein and Schwartz, 1979; Hoek and Brown, 1980; Duddeck and Erdmann, 1984; Barret and Mccreath, 1995) along with the use of numerical analyses (finite, boundary, discrete, hybrid, and finite difference methods) can be used simultaneously in the various phases of analysis and design of shotcrete as ground support.

Shotcrete support design in tunnels strongly relies on the assumed type of rock failure mechanism that governs loading environment and shotcrete behavior, in which the latter can be classified in adhesion failure, bending failure, direct shear failure, punching shear failure, compressive failure, and tensile failure (Barret and Mccreath, 1995). The fundamental goal of shotcrete design is to create a self-supporting arch, comprised of shotcrete and other support components such as rock bolts, grouted rebars, meshes, and cables to resist the imposed loads and deformations. In particular, in tunnels located at large depths, the rock support

* Corresponding author. Diagonal Las Torres 2640, Peñalolén, Santiago, Chile.
E-mail addresses: ricardo.moffat@uai.cl (R. Moffat), cjadue@petrus.cl (C. Jadue), jbeltran@ing.uchile.cl (J.F. Beltran), riherrer@ing.uchile.cl (R. Herrera).

http://dx.doi.org/10.1016/j.geotexmem.2017.01.007
0266-1144/

system should allow the occurrence of an admissible displacement of the tunnel walls while preventing the collapse of the tunnel. In this condition, the relevant characteristics of the shotcrete to consider are: its deformability at the maximum displacement, and the strength at that displacement. In this case, the design does not look for a rigid support that maintains the original stress condition around the tunnel, but allows deformation transferring energy from the rock to the shotcrete lining (Matsumoto and Nishioka, 1992).

Following the idea that the shotcrete lining gradually deforms and balances the ground movements after excavation of a tunnel, the popular NATM (New Austrian Tunneling Method) was first conceptualized and used in the Tauern Tunnel in Austria in 1972 and later related to the concept of ground reaction curve (Brown et al., 1983) as shown in Fig. 1. Depending on the stress-displacement behavior or capacity to absorb energy of the reinforcement on the tunnel, there can be three different situations: Case A: the capacity of the support system is high enough to stop the deformation of the tunnel at low displacements (δ1); Case B: the support system has the capacity to stabilize the tunnel at large displacement (δ2) when the ground reaction curve has lower energy and pressure; and Case C: the support system does not have the capacity to stabilize the tunnel walls. It is important to point out that Case B and C have the same peak strength; however only Case B is able to generate a safe condition even if large displacements may be required. The principles of this method have been applied in different projects around the world. The design of fiber reinforced shotcrete as a primary support for a 10 m diameter tunnel on weak rock (Jovicic et al., 2009) and the idea that mine openings have to tolerate large deformations as a result of changes in stress due to mining activity (Vandewalle, 1998) are some examples of the application of this principle. It is important to point out that in this last application, it was emphasized that the ductility of the shotcrete lining can be measured by testing the moment bearing capacity of a shotcrete beam specimen and deducing an energy absorption capacity from the load displacement curve.

Following the aforementioned idea of energy absorption capacity, a shotcrete property utilized for design purposes in underground mines is based on what has been called toughness (post-crack ductility). It is mentioned in (Papworth, 2002) that it is necessary to consider toughness requirement in widely used design tools such as the Barton Chart and also recommended the use of round panel tests (such as ASTM C1550, 2012) where central deflection is measured when a load is applied to the disc (see Fig. 2) for its computation. A modified Barton chart is proposed where energy absorption deduced from testing is considered in order to determine the necessary shotcrete thickness. This would allow considering different types of shotcrete reinforcement in the design of shotcrete for underground rock tunnels. Consequently, reinforced shotcrete has been increasing its importance in terms of its capability to absorb larger amount of energy or displacement of the rock.

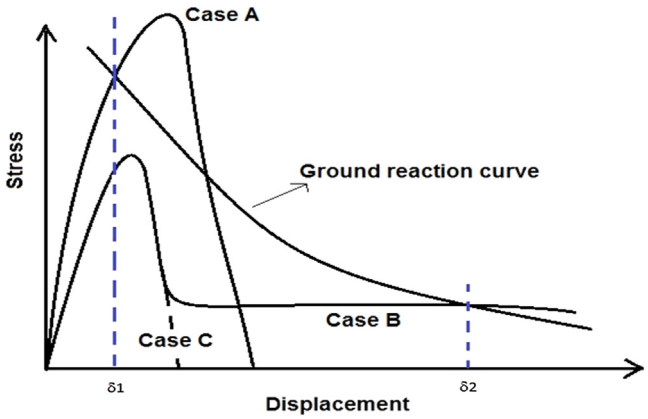

Fig. 1. Interaction between ground reaction curve and support performance.

1.1. Geosynthetics as reinforcement

Many studies have reported the beneficial effect of the geosynthetics reinforcements in geotechnical applications; construction of embankments over soft foundations soils (Fun and Hsieh, 2011; Rowe and Taechakumthorn, 2011; Karim et al., 2011; Zhuang and Wang, 2015; Chen et al., 2016); mitigation of hazardous effect of repeated loading on buried pipes (lifelines) (Mehrjardi et al., 2012; Corey et al., 2014; Hedge and Sitharam, 2015, 2016); improvement of pavement and rail track performance (Indraratna et al., 2010; Roodi and Zornberg, 2012; Zornberg, 2012; Yang and Han, 2013; Wu et al., 2015); stone columns improvement with geogrid encasement (Dash and Bora, 2013; Almeida et al., 2014; Hong et al., 2016); and stabilization of earthen walls and slopes (Silva et al., 2011; Yang et al., 2012).

In the particular case of reinforced shotcrete design, several experimental studies (Kirsten, 1998; Cengiz and Turanli, 2004; Morton et al., 2009; Mardookhpour, 2012; Kaufmann et al., 2013; Deng et al., 2016) have been conducted to evaluate the impact of using synthetic materials as reinforcement on shotcrete properties. Similar studies have been performed for reinforced concrete using polymers (El-Sayed et al., 2012; Mahmoud and El-Salakawy, 2015, 2016; Serna et al., 2016). These studies have shown that synthetic materials significantly improve ductility in the post-crack region and flexural toughness of plain shotcrete, offering an alternative solution to the traditional steel reinforcement (fibers and mesh). For example, a shotcrete reinforced with 0.78% of polypropylene fibers (volume occupied by the fibers in 1 m^3 of shotcrete) showed better post-crack performance (in terms of peak load and toughness) than a 0.45% steel fiber reinforced shotcrete, based on the results given by a panel test (Cengiz and Turanli, 2004). In addition to provide comparable post-crack performance to steel fiber reinforced shotcrete and increase shotcrete layer built-up thickness relative to the use of steel fibers (Dufour et al., 2006), synthetic materials are highly resistant to corrosion and they are safer, lighter, and easier to handle than steel (Yin et al., 2015).

Regarding the use of synthetic materials to reinforce shotcrete, experimental works have been mainly focused on the effect of macro synthetic fiber (polypropylene, aramid, high-density polyethylene, polyethylene terephthalate) on post-crack shotcrete performance. This performance is mainly influenced by the rebound of the fiber and material and also by the amount, distribution and orientation of the fibers, parameters that are determined by the application technique of the composite (Kaufmann et al., 2013). Although mixing processes have been improved and fiber manufacturers have developed new fiber geometries to prevent fibers clumps from forming, fiber clumps can still be observed in shotcrete, decreasing the toughness performance of the composite (Fig. 2).

Similar to synthetic macro fiber, geogrids and geotextiles could also be considered as a non-corroding alternative to steel mesh and fibers, but they eliminate the problem of clumps. In addition, geogrid and geotextile reinforcement may be oriented favorably with respect to the expected forces on the shotcrete in order to bridge the tensile forces to control crack development.

In this paper, an experimental study of the behavior of shotcrete reinforced with different types of geosynthetics is presented. A series of 35 ASTM C1550 round panel tests were carried out on

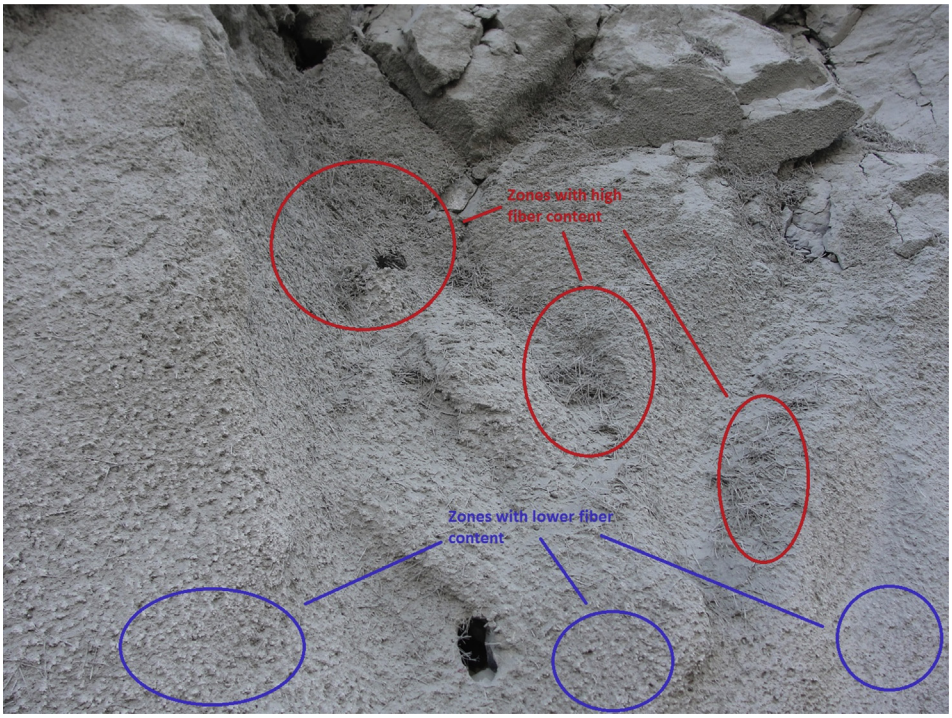

Fig. 2. Uneven distribution of fibers in fiber-reinforced shotcrete.

shotcrete panels reinforced with geogrids and geotextiles with different mechanical properties. The behavior of the reinforced shotcrete has been evaluated in terms of shear strength and energy absorption. Tests are also performed on plain shotcrete and shotcrete reinforced with steel mesh round panels for comparisons purposes.

2. Experimental device and testing procedures

Shotcrete performance can be evaluated in many ways, but the ability of reinforced shotcrete to retain ductility (measured as toughness) after localized cracking developed in the shotcrete matrix, is generally recognized as being important to the successful use of the composite (Bernard, 2008). The standard test method ASTM C1550 was developed to quantify the influence of reinforcement on shotcrete. In this study, the aforementioned test is used to compare the behavior of shotcrete reinforced with different types of geosynthetics. The performance of different reinforced shotcrete is compared in terms of energy absorbed at a 40 mm disc deflection, as it will be defined later in this paper. During the tests, round shotcrete panels of 80 cm diameter and approximately 75 mm thickness are subjected to a central point load while supported on three symmetrically arranged pivots (see Fig. 3). The load is applied at the center of the shotcrete panel using a standard rate of displacement and the load and deflection are measured by an automated acquisition system. Energy absorbed is calculated as the area below the load versus displacement curve. All the panels were tested 21 days after being cast in the lab.

2.1. Characteristics of reinforcement materials

Tests reported in this paper correspond to round shotcrete panels with and without reinforcement. The reinforcements considered in these tests correspond to steel mesh, geosynthetics grids, and geotextiles of different types. The steel mesh is fabricated from AT56-50H steel with a wire mesh diameter of 4.2 mm, spaced at 10 cm in both directions. Geosynthetics in different geogrid and geotextiles are described in Table 1.

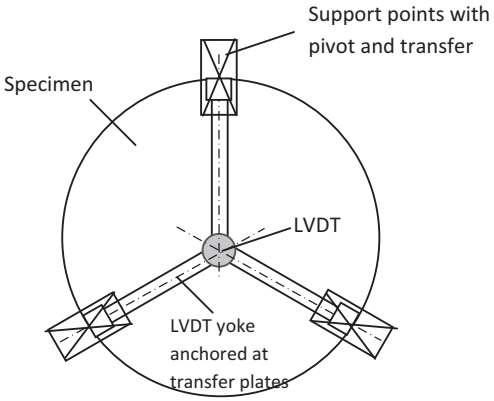

Fig. 3. Schematic of plan view of shotcrete disc and support points (ASTM C1550, 2012).

Shotcrete was prepared in the laboratory using cement, fine sand, a high range water reducer additive (Sika® Viscocrete® 5100 CL) and water. The dosage of each element is similar to the one used in mining activities.

2.2. Fabrication of panels

The specimens were fabricated in the laboratory using a hand fed concrete mixer. The procedure to elaborate the shotcrete was the following:

- Feed the cement and fine aggregate (sand) and mix until obtaining a homogeneous appearance.
- Add required water in 4 equal parts.

Table 1
Geosynthetics tested as shotcrete reinforcement.

Code	Type	Stiffness @ x% strain (kN/m)	Ultimate tensile strength (kN/m)	x%	Opening size s (mm)
WM1	Wiremesh	N.A.	N.A.	N.A.	100
UN1	Uniaxialgeogrid	1200	70	0.50%	152
UN2	Uniaxialgeogrid	1200	70	0.50%	152
TR1	Three-directional geogrid	300	N.A.	0.50%	40
TR2	Three-directional geogrid	350	N.A.	0.50%	60
BI1	Bi-directional geogrid	370	20	2%	38
BI2	Bi-directional geogrid	540	30	2%	38
BI3	Bi-directional geogrid	300	19.2	2%	25
BI4	PVC bi-directional geogrid	N.A.	N.A.	N.A.	40
GT1	Non-woven geotextile	N.A.	8	50%	0.15
GT2	Non-woven geotextile	N.A.	9	50%	0.15
GT3	Non-woven geotextile	N.A.	15	50%	0.15

– Slowly add the admixtures to distribute them as evenly as possible in the mix.
– Mix until achieving the desired workability.

Water reduction admixture *Viscocrete* 5100 (Sika) and superplasticizer *Glenium* 355C (BASF) were used, corresponding to 1% of the cement weight. Fig. 4 shows the mix inside the mixer.

The specimens were fabricated following the requirements of Section 7.1 of ASTM C1550, in terms of mold size, mix placement procedure, curing conditions, and test execution. The steel mold was circular with a diameter of 800 mm ± 10 mm and a wall height of 75 mm ± 10 mm (see Fig. 5). The position of the reinforcement was marked on the mold wall. For the tests reported here the reinforcement was placed at one third of the wall height.

A debonding agent was first applied to the bottom and walls of the mold. Then, a first layer of shotcrete was placed at the bottom of the mold up to the location of the reinforcement, followed by the placement of the reinforcement. Finally, a second layer of shotcrete was placed filling the mold completely (see Fig. 6). The exposed surface of the specimen was given a smooth finish before hardening of the mix had started.

The molds were cast and stored indoors, covered with plastic wrap, and let stand curing for at least 21 days to achieve a representative strength before testing. After the 21 days, the specimens were removed from the molds and placed in the test setup.

3. Experimental results

In total, thirty five tests on shotcrete with and without reinforcement were carried out in this experimental study. Tests on unreinforced and wire mesh reinforced shotcrete are used as references as they are common in mining and civil engineering applications. Test responses show marked peak strength followed by a rapid decrease of strength. Fig. 7 shows the behavior of unreinforced shotcrete in which a significant variability in peak load between the tests is obtained. It is believed that this is the result of deficiencies during the casting of the panel or the creation of microfractures during transportation of the shotcrete panel. The energy absorbed by the unreinforced shotcrete panels (E_{un}) is in average 18 J. This energy value will be used as a base of comparison to minimize the effect of small differences produced by changes in shotcrete strength due to dosage.

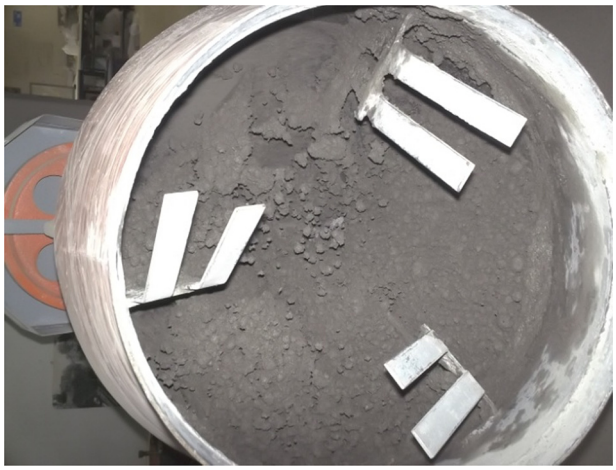

Fig. 4. Shotcrete mix elaboration.

The load-deformation response of the shotcrete panels with wire mesh reinforcement is presented in Fig. 8, in which ϕ corresponds to the diameter of the wires, equal to 4.2 mm. A small difference in the energy absorbed was observed between the two tests, which can be explained by the difference in orientation of the mesh with respect to the support points during each test. From this figure, it can be derived that the energy absorbed up to 40 mm of deflection increased in 1700% in the first test with wire mesh and in 1790% in the second test with respect to E_{un}. Although both tests gave similar values of energy absorbed, their responses are different. One of the tests apparently reaches its peak load for a central displacement of the panel equal to 12 mm after which the load-deflection curve exhibits a practically steady drop in strength as a function of the aforementioned central displacement. In contrast, the other test reported a relatively steep and sudden drop from the first peak load (crack of the shotcrete matrix), reached at a panel central deflection equal to 2.5 mm, to a strength value approximately equal to 40% of this first peak load. After this initial drop in strength, the specimen regains strength and a second peak load is observed, whose value is quite similar to the first peak load, at a central deflection of the panel close to 20 mm. After this second peak load, a steady drop in strength as function of panel deflection is exhibited by the load-deflection curve.

The responses of the specimens reinforced with three-directional geogrid are shown in Figs. 9 and 10. The differences between these two types of geogrid are the stiffness and opening size values as reported in Table 1. Reinforced shotcrete specimens with these two types of geogrid have similar behavior when the load-deflection curves are compared: after the first peak load (crack of the shotcrete matrix), a rapid decrease in strength is developed (similar to the one presented for the plain shotcrete response) up to a load value approximately equal to 20% of the first peak after which the reinforced shotcrete gains strength reaching a second peak load value approximately equal to 40% of the first peak load. After this second peak load value, the strength of the reinforced shotcrete decreases as the central deflection of the specimens

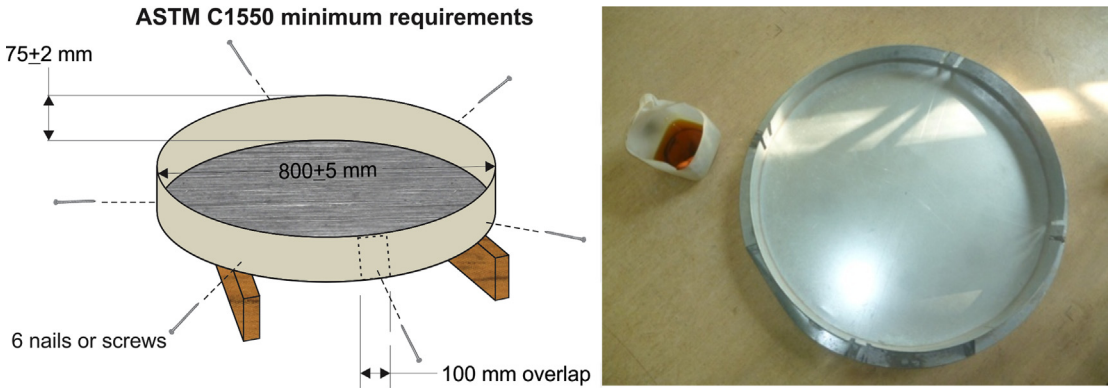

Fig. 5. Steel mold used, as per ASTM C1550 (2012).

Fig. 6. Fabrication of test specimen with geogrid.

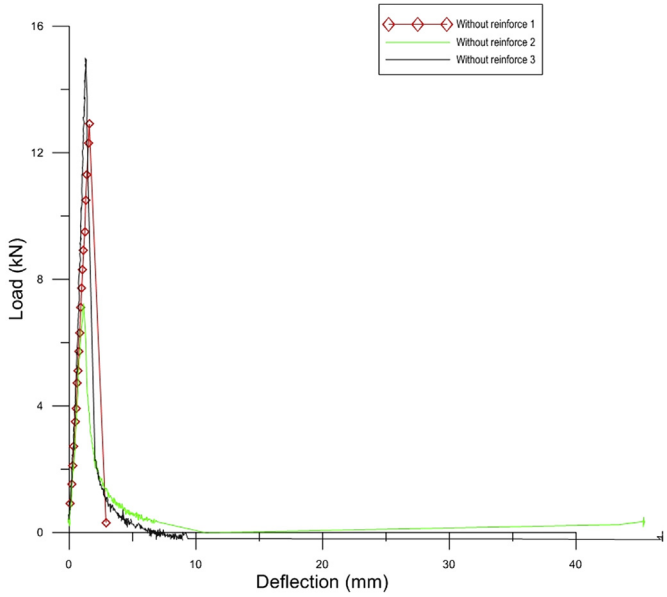

Fig. 7. Load deflection curve for unreinforced shotcrete.

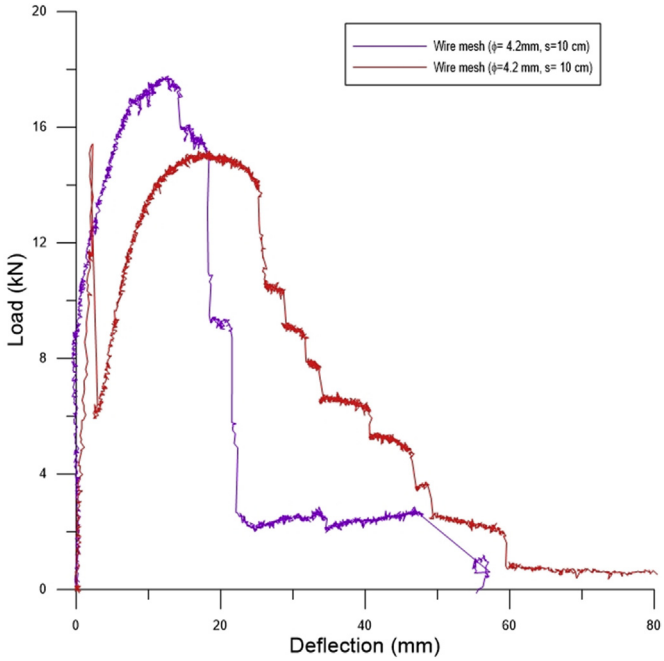

Fig. 8. Load deflection curve for shotcrete reinforced with wire mesh.

increases. This study also considered the experimental evaluation of using bi-directional geogrids (BI1, BI2, and BI3 in Table 1) to reinforce shotcrete. Experimental results were similar to the ones obtained for the shotcrete specimens reinforced with three-directional geogrids, hence the results are not included here, but they can be found in (Jadue, 2013).

In the case of specimens reinforced with two similar uniaxial geogrids, minor differences can be observed in the load-deflection curves, due to the preferential direction of the grid (see Figs. 11 and 12). Post-peak (after the first peak load) behavior differs from the one obtained for the three-directional geogrid case because, although the reinforced shotcrete specimens exhibit a decrease in strength after the onset of shotcrete matrix cracking, it is not as

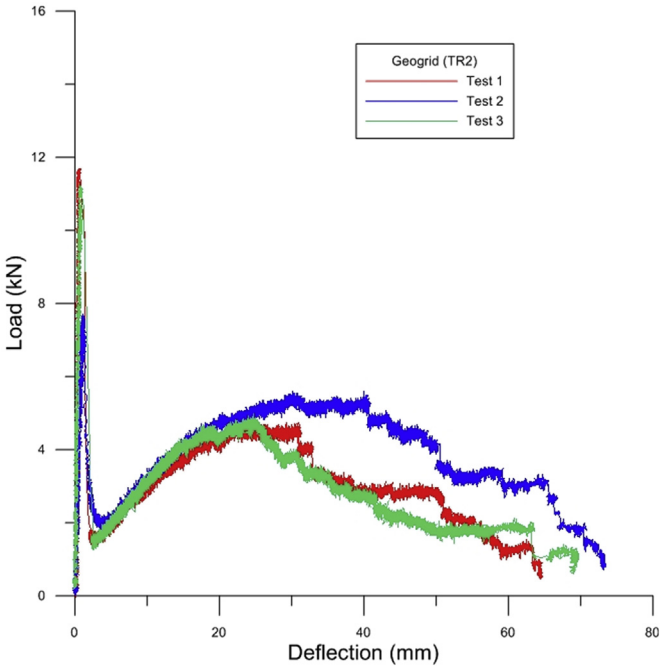

Fig. 9. Load deflection curves for shotcrete reinforced with geogrid TR2.

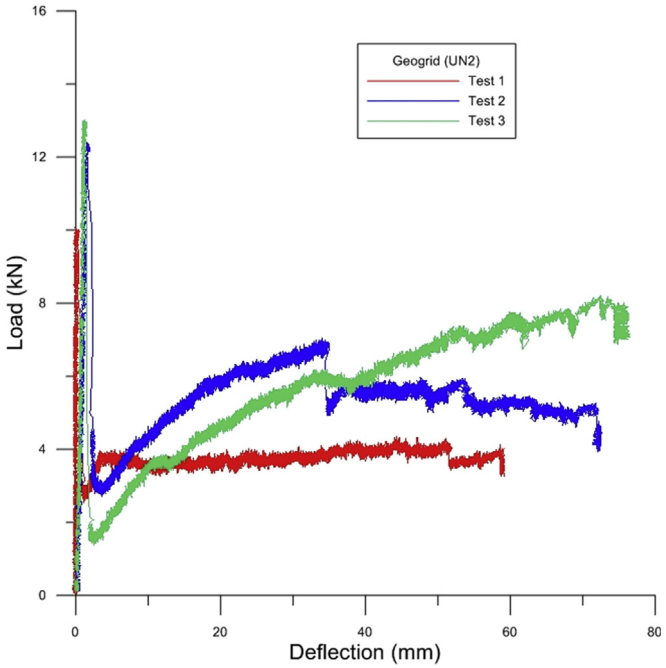

Fig. 11. Load deflection curves for shotcrete reinforced with geogrid UN2.

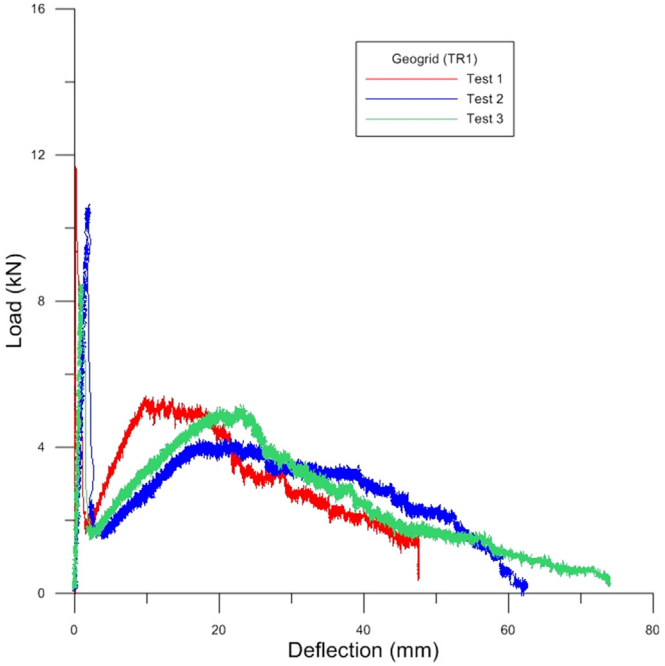

Fig. 10. Load deflection curves for shotcrete reinforced with geogrid TR1.

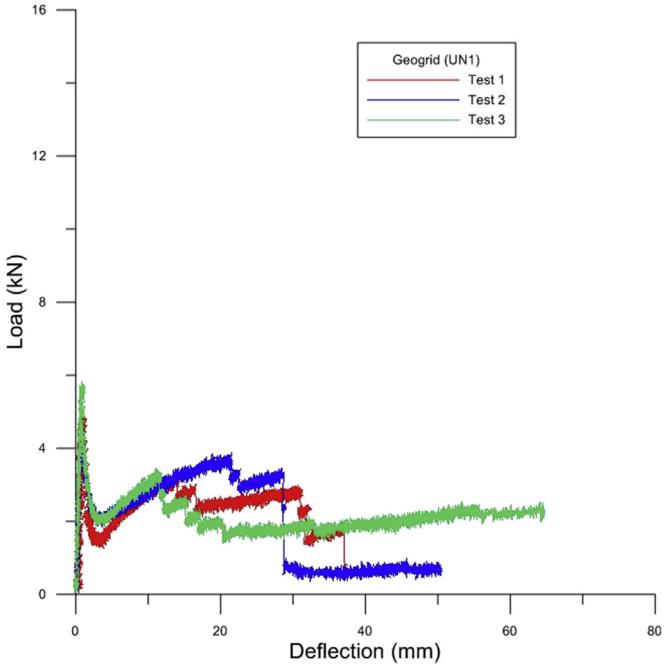

Fig. 12. Load deflection curves for shotcrete reinforced with uniaxial geogrid UN1.

steep as in the case of three-directional geogrids. The minimum average strength carried by the reinforced shotcrete specimens, before regaining strength as the central panel deflections increase, ranges from 23% to 37% of the first peak load values. In addition, it is not possible to establish a second peak load for all the specimens tested after they regain strength after initial cracking of the shotcrete matrix. When the specimen response exhibits a second peak load, this value is about 60% of the first peak value, amount greater than the one developed for the three-directional geogrid case.

Shotcrete reinforced with geotextiles (GT1, GT2, and GT3 in Table 1) did not perform as expected. In half of the specimens the geotextile debonded from the shotcrete as shown in Fig. 13 for the case of geotextile GT1. In all these cases, the energy absorbed was less than E_{un}. For the cases in which no debonding occurred, the energy absorbed by the specimens is reported in Fig. 11 along with the values of the same parameter (toughness) of the other types of reinforcement material evaluated in this study as later explained and discussed.

As seen in Figs. 7–12, the load-deflection response, especially after of the onset of shotcrete cracking (the so-called post-peak

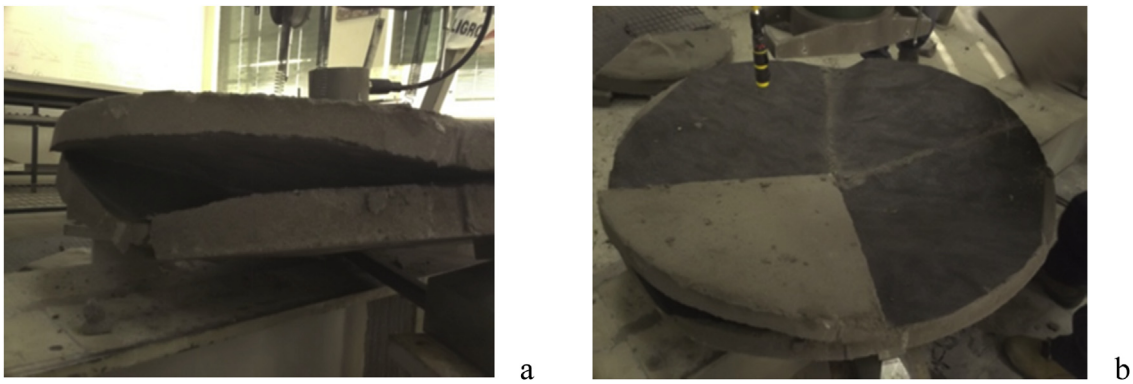

Fig. 13. Debonding of geotextile GT1 from the shotcrete.

response), is distinctly different between the reinforcements used in this study. The relative stiffness between shotcrete and the reinforcements plays a big role on post-peak response of the reinforced shotcrete; thus, the selection of the type of reinforcement will depend on the specific project requirements. Considering Fig. 1 as a generic example, for the ground reaction curve shown, only materials A and B could be used. Even if both materials can absorb similar amount of energy, if the application calls for avoiding large displacements, material A would be better suited, whereas if larger displacements are allowed, material B could be a better option.

Lastly, Fig. 14 shows the summary of the energy absorbed, for a value of the central deflection of the specimens arbitrarily set to 40 mm, for the different types of reinforcement used. All the values are normalized by the energy absorbed by the unreinforced shotcrete disc (E_{un}). In all cases, a significant improvement is observed on the energy absorption capacity, ranging from 5 to 20 times E_{un}. This improvement in energy absorption capacity is in most cases larger than the average value provided by shotcrete reinforced with polypropylene and steel fibers (Yin et al., 2015), shown as dashed line in Fig. 14.

Shotcrete reinforced with a conventional steel wire mesh has the highest energy absorption at 40 mm of central deflection. However, the energy absorbed by the bi-directional geogrid specimens (identified in Table 1) is comparable to that of the wire mesh reinforced panels (approximately 85%).

Three-directional and uniaxial grid reinforced panels absorb similar amounts of energy. Although shotcrete panels reinforced with geotextiles that did not show a debonding process have less capacity to absorb energy than the ones reinforced with three-directional and uniaxial grids, they have comparable (and some panels greater) capacity to absorb energy than the panels reinforced with 0.45% and 0.78% steel and polypropylene fibers respectively. As such, further investigation is needed on the construction and configuration of shotcrete panels reinforced with geotextiles in order to obtain reliable experimental results and ensure an adequate adhesion between shotcrete and geotextiles during panel fabrication process to avoid premature debonding.

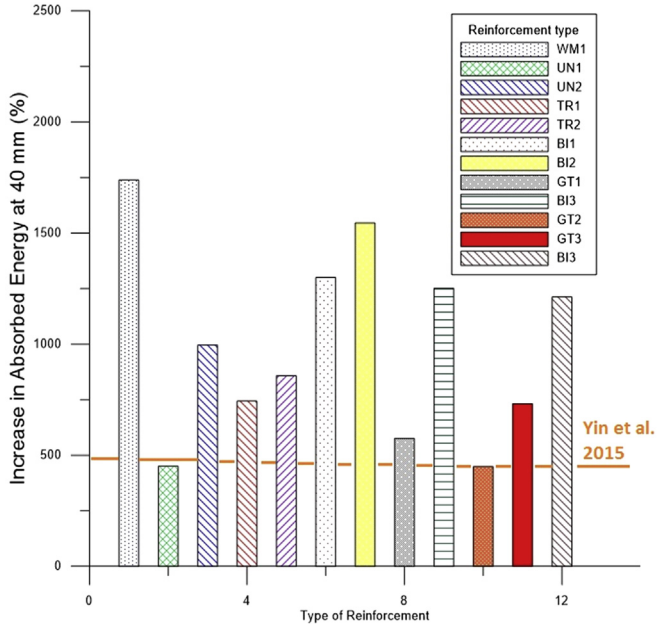

Fig. 14. Percentage increase in absorbed energy relative to unreinforced shotcrete case.

4. Conclusions and implications in design

The following conclusions are based on the results on ASTM C-1550 tests performed on unreinforced shotcrete, wire mesh reinforced shotcrete and shotcrete reinforced with different geosynthetics:

1. All the reinforcements tested in this study provided a significant increase in the energy absorbed at 40 mm of deflection, ranging between 5 and 20 times the energy of the unreinforced specimens, with the exception of geotextile specimens where debonding occurred.
2. Peak strength is not significantly affected by the type of reinforcement used. Peak strength is attained due to the strength of the shotcrete itself with little contribution from the reinforcement. The peak strength occurs at small displacements (2–3 mm), before cracks are noticed in the shotcrete.
3. Uniaxial, bi-directional, and three-directional geogrids are able to maintain a proper bond with the shotcrete. Based on the experience of fabrication of the discs in the laboratory, it is believed that their installation in real tunnel projects will be easier than installing commonly used wire mesh, because of its lighter weight and packability.
4. Wire mesh reinforced shotcrete absorbed the largest amount of energy of all types of reinforcement. However, bi-directional geogrids tested showed a similar energy absorption level and due to the nature of the material it is expected that they would stay in better condition than steel mesh under moist environments usually found in tunnels.
5. Uniaxial and three-directional geogrids also showed an adequate capacity to absorb energy. Their response, as well as

that of the bi-directional geogrids, is very homogeneous according to the tests performed. It must be noted that other three-directional geogrids could provide improved performance and therefore further investigation should be conducted.

6. Geotextiles debonded from the shotcrete in a large percentage of the tests. Although the tests on geotextiles that could be completed showed an important increase of energy absorption (in the order of 500%) with respect to unreinforced shotcrete, it is believed this situation will be critical in real installation on the field. Therefore, based on these laboratory results, further investigation is needed on the use of geotextiles as reinforcement for shotcrete.

References

Almeida, M., Hosseinpour, I., Riccio, M., Alexiew, D., 2014. Behavior of geotextile-encased granular columns supporting test embankment on soft deposit. J. Geotech. Geoenviron. Eng. 141, 04014116–1-9.

Ansell, A., 2010. Structural behaviour of shotcrete on irregular hard rock surfaces. In: Shotcrete: Elements of a System. CRC Press/Balkema, Leiden, The Netherlands.

ASTM C1550, 2012. Standard Test for Flexural Toughness of Fiber Reinforced Concrete (Using Centrally Loaded Round Panel). ASTM C1550 – 12a, West Conshohocken, Pennsylvania, USA.

Austin, S., Robins, P., 1995. Sprayed Concrete: Properties, Design and Applications. Whittles Publishing, Caithness, Scotland.

Barret, S., Mccreath, D., 1995. Shotcrete support design in blocky ground: towards a deterministic approach. Tunn. Undergr. Sp. Tech. 10 (1), 79–89.

Barton, N., Lien, R., Lunde, J., 1974. Engineering classification of rock masses for the design of tunnel support. Rock Mech. 6 (4), 189–236.

Bernard, E., 2008. Embrittlement of fibre reinforced shotcrete. Shotcrete 10, 16–21.

Bieniawski, Z.T., 1994. Rock Mechanics Design in Mining and Tunnelling. Balkema, Rotterdam.

Brown, E., Bray, J., Ladanyi, B., Hoek, E., 1983. Ground response curves for rock tunnels. J. Geotech. Eng. 109 (1), 15–39.

Cengiz, O., Turanli, L., 2004. Comparative evaluation of steel mesh, steel fibre and high-performance polypropilene reinforced shotcrete in panel test. Cem. Concr. Res. 34, 1357–1364.

Chen, R.P., Wang, Y.W., Ye, X.W., Bian, X.C., Dong, X.P., 2016. Tensile force of geogrids embedded in-pile supported reinforced embankment: a full-scale experimental study. Geotext. Geomembr. 44, 157–169.

Corey, R., Han, J., Khatri, D.K., Parsons, R.L., 2014. Laboratory study on geosynthetic protection of buried steel-reinforced HDPE pipes from static loading. J. Geotech. Geoenviron. Eng. 140 (6), 04014019.

Dash, S.K., Bora, M.C., 2013. Influence of geosynthetic encasement on the performance of stone columns floating in in soft clay. Can. Geotech. J. 50 (7), 754–765.

Deng, Z., Shi, F., Yin, S., Tuladhar, R., 2016. Characterization of macro polyolefin fibre reinforcement concrete through round determinate panel test. Constr. Build. Mat. 15, 229–235.

Duddeck, H., Erdmann, J., 1984. Structural design models for tunnels. Int. J. Rock Mech. Min. 9, 5–6.

Dufour, J., Trottier, J., Forgeron, D., 2006. Behaviour and performance of monofilament macro-synthetic fibres in dry-mix shotcrete. In: Proceedings of the Shotcrete for Underground Support X, Whistler, BC, Canada.

Einstein, H., Schwartz, W., 1979. Simplified analysis for tunnel supports. J. Geotech. Eng. 105 (4), 499–518.

El-Sayed, A.K., El-Salakawy, E.F., Benmokrane, B., 2012. Shear strength of fibre-reinforced polymer reinforced concrete deep beams without web reinforcement. Can. J. Civil Eng 39 (5), 546–555.

Franzen, T., 1992. Shotcrete for underground support: a State-of-the-art report with focus on steel-fibre reinforcement. Tunn. Undergr. Sp. Tech. 7 (4), 383–391.

Fun, C., Hsieh, C., 2011. The mechanical behavior and design concerns for a hybrid reinforced earth embankment built in limited width adjacent to a slope. Comp. Geotech 38, 233–247.

Galli, G., Grimaldi, A., Leonardi, A., 2004. Three-dimensional modeling of tunnel excavation and lining. Comp. Geotech. 31, 171–183.

Hedge, A., Sitharam, T., 2015. Experimental and numerical studies on protection of buried pipelines and underground utilities using geocells. Geotext. Geomembr. 43, 372–381.

Hedge, A., Sitharam, T., 2016. Behaviour of geocell reinforced soft clay bed subjected to incremental cyclic loading. Geomech. Eng. 10, 405–422.

Hoek, E., Brown, E., 1980. Underground Excavation in Rock. Institution of Mining and Metallurgy, London, England.

Hoek, E., Kaiser, P., Bawden, W., 2000. Support of Underground Excavation in Hard Rock. CRC Press, Boca Raton, Florida, USA.

Hong, Y., Wu, C., Yu, Y., 2016. Model tests on geotextile-encased granular columns under 1-gand undrained conditions. Geotext. Geomembr. 44, 13–27.

Indraratna, B., Nimbalkar, S., Christie, D., Rujikiatkamjorn, C., Vinod, J., 2010. Field assessment of the performance of a ballasted rail track with and without geosynthetics. J. Geotech. Geoenviron. Eng. 136 (7), 907–917.

Jadue, C., 2013. Aplicación de geosintéticoscomorefuerzo de morter-oproyectadoensistemas de sostenimiento, Thesis to obtain the title of Civil Engineer. University of Valparaiso, Valparaiso, Chile.

Jovicic, V., Sstesic, J., Vukelic, Z., 2009. The application of fiber reinforced shotcrete as primary support for a tunnel in flysch. Tunn. Undergr. Sp. Tech. 24, 723–730.

Karim, M.R., Manivannan, G., Gnamendran, C.T., Lo, S.-C.R., 2011. Predicting the long-term performance of a geogrid-reinforced embankment on soft soil using two-dimensional finite element analysis. Can. Geotech. J. 48 (5), 741–753.

Kaufmann, J., Frech, K., Schuetz, P., Munch, B., 2013. Rebound and orientation of fibers in wet sprayed concrete applications. Constr. Build. Mat. 49, 15–22.

Kirsten, H., 1998. System ductility of long fiber reinforced shotcrete. J. South Afr. Inst. Min. Metall. March/April 93–104.

Mahmoud, K., El-Salakawy, E., 2015. Shear strength of glass fiber reinforced polymer-reinforced concrete continuous beams without transverse reinforcement. Can. J. Civ. Eng 42 (12), 1073–1082.

Mahmoud, K., El-Salakawy, E., 2016. Size effect on shear strength of glass fiber-reinforced polymer-reinforced concrete continuous beams. ACI Struct. J. 113, 125–134.

Malmgren, L., 2005. Interaction between Shotcrete and Rock-experimental and Numerical Study. PhD dissertation. Lulea University of Technology, Sweden.

Mardookhpour, A.R., 2012. Experimental evaluation of the effect of utilizing Geosynthetics on structural concrete beams strength. Emerg. Mater. Res. 1 (3), 136–139.

Matsumoto, Y., Nishioka, T., 1992. Theoretical Tunnel Mechanics. University of Tokyo Press, Tokyo, Japan.

Mehrjardi, G., Tafreshi, S., Dawson, A., 2012. Combined use of geocell reinforcement and rubbersoil mixtures to improve performance of buried pipes. Geotext. Geomembr. 34, 116–130.

Morton, E., Villaescusa, E., Thompson, A., 2009. Determination of energy absorption capabilities of large scale shotcrete panels. In: Proceedings of the ECI Conference on Shotcrete for Underground Support XI, Davos, Switzerland.

Palmstrom, A., 1996. Characterizing rock masses by the RMI for use in practical rock engineering, part 2: some practical applications of the rock mass index (RMI). Tunn. Undergr. Sp. Tech. 11 (3), 287–303.

Papworth, F., 2002. Design guidelines for the use of fiber-reinforced shotcrete in ground support. In: Proceedings of the 27th Conference on Our World in Concrete & Structures, Singapore, pp. 429–436.

Roodi, G., Zornberg, J., 2012. Effect of geosynthetic reinforcements on mitigation of environmentally induced cracks in pavements. In: Proceedings of the 5th European Geosynthetic Congress, EuroGeo 5, Valencia, Spain.

Rowe, R., Taechakumthorn, C., 2011. Design of reinforced embankments on soft clay deposits considering the viscosity of both foundation and reinforcement. Geotext. Geomembr. 29, 448–461.

Serna, P., Martí-Vargas, J.R., Bossio, M., Zerbino, R., 2016. Creep and residual properties of cracked macro-synthetic fibre reinforced concretes. Mag. Concr. Res. 68 (4), 197–207.

Silva, C., Lopes, M., Caldeira, L., 2011. Earth pressure coefficients for design of geosynthetic reinforced soil structures. Geotext. Geomembr. 29, 491–501.

The British Tunneling Society, The Institution of Civil Engineers, 2004. Tunnel Lining Design Guide. Thomas Telford, London, England.

Vandewalle, M., 1998. The use of steel fibre reinforced shotcrete for the support of mine openings. J. South Afr. Inst. Min. Metall. May/June 113–120.

Wood, A.M., 1975. The circular tunnel in elastic ground. Geotechnique 25 (1), 115–127.

Wu, H., Huang, B., Shu, X., Zhao, S., 2015. Evaluation of geogrid reinforcement effects on unbounded granular pavement base courses using loaded wheel tester. Geotext. Geomembr. 43, 462–469.

Yang, K., Zornberg, J., Liu, C., Lin, H., 2012. Stress distribution and development within geosynthetic-reinforced soil slopes. Geosynth. Int. 19, 62–78.

Yang, X., Han, J., 2013. Analytical model for resilient modulus and permanent deformation of geosynthetic-reinforced unbound granular material. J. Geotech. Geoenviron. Eng. 139, 1443–1453.

Yin, S., Tuladhar, R., Collister, T., Combe, M., Sivakugan, N., Deng, Z., 2015. Post-cracking performance of recycled polypropylene fibre in concrete. Constr. Build. Mat. 101, 1069–1077.

Zhuang, Y., Wang, K.Y., 2015. Three-dimensional behavior of biaxial geogrid in a piled embankment: numerical investigation. Can. Geotech. J. 52 (10), 1629–1635.

Zornberg, J., 2012. Geosynthetic-reinforced pavement systems. In: Proceedings of the 5th European Geosynthetic Congress, EuroGeo 5, Valencia, Spain.